Predicting thermal conductivity in filled polyurethane composites

Marian Janek [1*], *Stefan* Hardon[2], and *Jozef* Kudelcik[1]

[1]Department of Physics, Faculty of Electrical Engineering and Information Technology University of Zilina, Zilina, Slovakia

Abstract. Predicting the effective thermal conductivity of polymer composites is crucial for optimizing materials for demanding thermal management applications. This study focuses on Polyurethane (PU) composites (specifically VUKOL Magna Blue) with Boron Nitride (BN) admixtures, testing concentrations of pure polymer, 10 wt%, and 20 wt% BN. Experimental measurements demonstrated a significant increase in effective thermal conductivity, rising from 0.2 Wm^{-1} K^{-1} for pure PU to approximately 0.68 Wm^{-1} K^{-1} at 20 wt% BN. These measured results were subsequently compared with predictions derived from established theoretical models. Particular attention was paid to the influence of Thermal Boundary Resistance (TBR), which was incorporated into a modified version of the Maxwell-Eucken model to improve the prediction accuracy at the filler-matrix interface. For validation, Finite Element Method (FEM) simulations of heat distribution and transfer within the composites were also performed. The comparison between the experimental data, theoretical calculations, and FEM simulation results revealed varying degrees of agreement and highlighted the limits and strengths of each predictive method. The findings emphasize that for accurate predictions of the thermal behavior of PU composites, it is essential not only to carefully select the appropriate theoretical model but also to responsibly consider and quantify factors such as TBR and the specific characteristics of the filler.

1 Introduction

Thermal management has become a critical challenge in
the development of modern electronic devices. As components continue to miniaturize and power densities increase, the efficient dissipation of waste heat is essential to ensure reliability, performance, and longevity [1]. Polymer-based materials are widely used in electronic packaging, encapsulants, and thermal interface materials due to their low cost, light weight, ease of processing, and excellent dielectric strength. However, most intrinsic polymers, including PU, possess very low thermal conductivity (typically 0.1 – 0.3 Wm^{-1} K^{-1}), which acts as a significant thermal bottleneck in heat dissipation pathways [2]. Beyond thermal properties, the electrical behavior of filled composites is also of considerable interest; for instance, dielectric spectroscopy studies of hybrid nanofluids containing magnetite and fullerene nanoparticles have revealed favorable relaxation behavior and conductivity characteristics for electrical insulation applications [3].

To address this limitation, high-thermal-conductivity fillers are often incorporated into the polymer matrix to form composites. The incorporation of nano-fillers into polyurethane matrices has been shown to improve not only thermal conductivity but also overall thermal stability and aging resistance [4]. While metallic fillers (e.g., silver, copper) and carbon-based fillers (e.g., graphene, carbon nanotubes) offer exceptional thermal conductivity, their high electrical conductivity often limits their application in scenarios where electrical insulation is strictly required [5]. Consequently, ceramic fillers such as alumina (Al2O3), aluminum nitride (AlN), and boron ni-tride (BN) have garnered significant attention. Hexagonal BN (h–BN), in particular, is often referred to as ”white graphite” due to its layered structure and lubricating properties. It offers a unique combination of high thermal conductivity (300 – 600 Wm^{-1} K^{-1} in the basal plane), high electrical resistivity, and low dielectric constant, making it an ideal candidate for next-generation electronic packaging applications [6].

The effective thermal conductivity of such composites depends on a multitude of factors, including filler loading, particle size, and the quality of the filler-matrix interface. However, the performance of these composites is often severely limited by the Thermal Boundary Resistance (TBR),

* Corresponding author: marian.janek@uniza.sk

also known as Kapitza resistance, at the polymer-filler interface. This resistance arises from phonon scattering due to the acoustic mismatch between the rigid ceramic filler and the soft polymer matrix, as well as voids or defects at the interface [7].

Predicting the thermal performance of these composites is complex. Classical effective medium theories, such as the Maxwell-Eucken model [8], often fail to account for non-spherical particle shapes and interfacial resistance accurately. The Nan et al. model [7] provides a more rigorous treatment by incorporating depolarization factors for ellipsoidal inclusions and direction-dependent interfacial thermal resistance. FEM simulations offer a powerful alternative, allowing for the direct solution of heat conduction equations on realistic microstructures, thereby providing deeper insights into the heat flux distribution and the impact of particle arrangement.

In this study, we investigate the thermal conductivity of PU composites filled with BN particles. We present analysis comparing experimental results with analytical predictions (Maxwell-Eucken and Modified and enhanced Maxwell-Eucken based on Nan et al.) and 3D FEM simulations.

2 Experimental methodology

The thermal conductivity measurements were performed using a novel experimental setup developed by the authors [10]. The setup utilizes a transient heat pulse methodology, where a planar heating element acts as the heat source, positioned between two identical cylindrical samples of the material being investigated. These samples feature specific grooves to accommodate the heater and two NTC thermistors to measure temperatures at defined locations. The transient temperature response is recorded and analyzed to extract the thermal conductivity of the material.

This method offers several advantages, including cost-effectiveness, reliability, and the ability to measure materials with a wide range of thermal conductivities. To address challenges in identifying heat dissipation during testing, advanced inverse heat conduction problem approaches can be employed to simultaneously determine thermal conductivity and dissipation coefficients [9]. The measurement uncertainty was determined to be ±0.02 $Wm^{-1} K^{-1}$. For detailed information on the measurement principle, calibration procedure, and validation, the reader is referred to Ref. [10].

3 Theoretical framework

The thermal conductivity of composite materials is a com-plex property governed by the intrinsic properties of the constituents, their volume fractions, the geometry of the filler particles, and the nature of the interface between the filler and the matrix. In this section, we outline the models employed, emphasizing the common parametrization that enables direct comparison. The Maxwell–Eucken model was selected as the classical baseline owing to its simplicity and widespread use for dilute particulate composites with spherical inclusions. The Nan et al. effective medium framework was subsequently adopted because it rigorously extends the Maxwell–Eucken formulation to non-spherical particles and explicitly accounts for interfacial thermal resistance, without introducing additional free parameters beyond those with clear physical motivation. The empirical connectivity enhancement was added only after confirming that mean-field theory alone cannot reproduce the accelerated increase observed experimentally at higher filler loadings.

3.1 Thermal Boundary Resistance

Heat transport in non-metallic solids is primarily conducted by phonons. At the interface between two dissimilar materials, such as a polymer and a ceramic filler, a discontinuity in the vibrational density of states leads to phonon scattering.

This phenomenon manifests as a temperature jump ΔT across the interface, characterized by the TBR, or Kapitza resistance (Rbd) [11].

To incorporate this interfacial effect into continuum models, we employ the ”Effective Particle Conductivity” (keff) approach. This method treats the filler particle and its surrounding resistive interface as a single effective inclusion with reduced conductivity. For a particle with characteristic length L_{char} and bulk conductivity k_{bulk}, k_{eff} is given by:

$$k_{eff} = \frac{L_{char}}{\frac{L_{char}}{k_{bulk}} + 2R_{bd}} \quad (1)$$

Where $L_{char} = 2r/AR$ for particles with radius r and aspect ratio AR. The interfacial resistance R_{bd} is defined as t_{int}/k_{int}, where t_{int} is the interphase thickness and k_{int} is the interphase conductivity.

Throughout this study, both analytical and numerical models employ identical material parameters: equivalent particle radius $r = 5.0$ µm, bulk filler conductivity k_{bulk} = 700 $Wm^{-1} K^{-1}$ matrix conductivity k_m = 0.21 $Wm^{-1} K^{-1}$ (polyurethane), interphase thickness t_{int} = 2.5 nm, and interphase

conductivity k_{int} = 0.25 $Wm^{-1} K^{-1}$. This yields R_{bd} = 1.0 × 10^{-8} $m^2 KW^{-1}$, within the typical range for polymer-ceramic interfaces. The TBR value was estimated based on values reported for analogous ceramic–polymer systems [7], [11]: TBR for polymer–ceramic interfaces is typically in the range 10^{-9}–10^{-7} $m^2 KW^{-1}$ [11], and R_{bd} = 1.0 × 10^{-8} m2 KW^{-1} is consistent with BN–polymer systems exhibiting moderate acoustic mismatch. The interphase thickness t_{int} = 2.5 nm reflects the typical extent of chain immobilization or orientational ordering in the polymer adjacent to the filler surface, while k_{int} = 0.25 $Wm^{-1} K^{-1}$ was set marginally above the bulk PU value to represent a region of partially ordered and densified polymer chains, in accordance with molecular-dynamics-based estimates for similar interfaces [11]. For aspect ratio AR = 1 (spherical particles), the characteristic length is L_{char} = 10.0 μm, yielding an effective filler conductivity of k_{eff} ≈ 77.8 $Wm^{-1} K^{-1}$, representing an 89% reduction from the bulk BN conductivity.

3.2 Maxwell-Eucken Model (Spherical Assumption)

The Maxwell-Eucken model is the fundamental theory for particulate composites, assuming a dilute suspension of non-interacting spherical particles [8]. The effective thermal conductivity is given by:

$$kc = km\frac{kf + 2km + 2\phi(kf - km)}{kf + 2km - \phi(kf - km)} \quad (2)$$

Where k_c is the composite conductivity, k_m is the matrix conductivity, k_f is the filler conductivity (either bulk or effective depending on TBR consideration), and ϕ is the volume fraction of the filler. This model serves as a baseline but ignores particle shape effects.

3.3 Modified Maxwell-Eucken model (Nan et al.)

To address the geometric limitations of the classical Maxwell-Eucken model for non-spherical particles with interfacial thermal resistance, we employ the effective medium theory developed by Nan et al. [7]. For spherical particles ($AR = 1$), this model simplifies to the classical Maxwell-Eucken formulation but with the effective particle conductivity k_{eff} from Eq. (1) replacing the bulk filler conductivity. This unified approach ensures that interfacial thermal resistance is consistently accounted for across all models.

3.4 Enhanced model with particle connectivity

Classical effective medium theories predict smooth, continuous increases in thermal conductivity with filler loading. However, experimental observations often reveal more rapid enhancement at higher filler concentrations, attributed to the formation of local conductive pathways through particle proximity. To capture this behavior, we augment the Nan et al. model with an empirical enhancement term:

$$k_c = k_{Nan}(\phi) + A \cdot (\phi - \phi_c)^t \; for \; \phi > \phi_c \quad (3)$$

Where $k_{Nan}(\phi)$ is the prediction from the Modified Maxwell-Eucken model, ϕ_c is the critical concentration (expressed in $w_t\%$), t is the exponent characterizing the transition, and A is the enhancement amplitude coefficient. These parameters were determined by fitting to experimental data: ϕ_c = 6.6 w_t%, t = 0.94, and A = 3.78 $Wm^{-1} K^{-1}$.

This enhanced formulation provides a seamless transition from dilute to concentrated regimes, capturing both the interfacial-resistance-limited behavior at low loadings and the connectivity-enhanced transport at high loadings.

4 Numerical implementation (FEM)

To explore the influence of microstructural geometry, we employed 3D FEM simulations using the identical parameter set as the theoretical models. This unified approach enables direct, quantitative comparison between analytical and numerical predictions.

4.1 Microstructure generation

The composite microstructure was modeled using a 3D Representative Volume Element (RVE). The Boron Nitride filler particles were modeled as spherical particles (aspect ratio AR = 1) with random positions. The RVE domain size was set to 26 × $R_{particle}$, where $R_{particle}$ = 5.0 μm is the particle radius (identical to the analytical models), corresponding to physical dimensions of approximately 130 μm.

The grid resolution was set to 603 hexahedral elements. To assess mesh sensitivity, preliminary simulations were carried out at 403, 603, and 803 element resolutions; the relative change in predicted effective thermal conductivity between the 603 and 803 grids was below 1%, confirming that the chosen resolution provides mesh-independent results at manageable computational cost. Coarser 403 grids showed deviations of up to 3% and were therefore

discarded. Particles were placed using a random sequential addition algorithm. The target volume fractions were ϕ = 5.97% and 12.5% corresponding to 10 and 20 w_t%, respectively, calculated using matrix density ρ_m = 1.2 g/cm^3 and filler density ρ_f = 2.1 g/cm^3 (consistent with the analytical models).

4.2 FEM formulation

The thermal problem was formulated as steady-state heat conduction governed by:

$$\nabla \cdot (k(x)\nabla T) = 0 \quad (4)$$

The domain was discretized using trilinear hexahedral (Q1) finite elements.

4.3 Material properties

Crucially, the FEM simulations employ the identical material parameters as the analytical models, ensuring consistent comparison. The matrix thermal conductivity was set to k_m = 0.21 Wm^{-1} K^{-1} (polyurethane). For the BN filler elements, the effective conductivity k_{eff} = 77.8 Wm^{-1} K^{-1} was used, calculated according to Eq. (1) with:

- Bulk filler conductivity: k_{bulk} = 700 Wm^{-1} K^{-1} (BN)
- Particle radius: r = 5.0 μm
- Aspect ratio: AR = 1 (spherical)
- Interphase thickness: t_{int} = 2.5 nm
- Interphase conductivity: k_{int} = 0.25 Wm^{-1} K^{-1}
- Thermal boundary resistance: R_{bd} = 10^{-8} m^2 KW^{-1}

This approach incorporates the interfacial thermal resistance directly into the element conductivity, maintaining consistency with the analytical treatment.

4.4 Boundary conditions and solution

Dirichlet boundary conditions were applied:

$$T(x = 0) = T_{hot} = 1,\ T(x = L) = T_{cold} = 0 \quad (5)$$

with adiabatic conditions on the remaining boundaries $(\partial T/\partial n = 0)$. This configuration is standard in RVE-based homogenization and ensures that the computed effective conductivity represents bulk composite behavior; the prescribed dimensionless temperature difference ΔT = 1 establishes a unit macroscopic temperature gradient along the x-direction, enabling direct extraction of the effective conductivity via Fourier's law. Periodic boundary conditions were considered but found to produce results within 0.5% of the Dirichlet configuration at the studied volume fractions, justifying the simpler choice.

The resulting sparse linear system was solved using the conjugate gradient method with diagonal preconditioning. The effective thermal conductivity was calculated from the total heat flux at the boundary:

$$k_c = \frac{Qtotal \cdot L}{A \cdot \Delta T} \quad (6)$$

Where L is the domain length and A = L2 is the cross-sectional area.

4.5 Statistical analysis

Multiple realizations were performed for each concentration to assess statistical variability: 1 realization for 0 w_t%, 20 realizations for 10 w_t%, and 60 realizations for 20 w_t%. Results are reported as mean ± standard error of the mean (SEM). Figure 1 shows a representative 2D slice through the 3D RVE microstructure for the 20 w_t% composite, illustrating the random distribution of spherical BN particles within the polyurethane matrix.

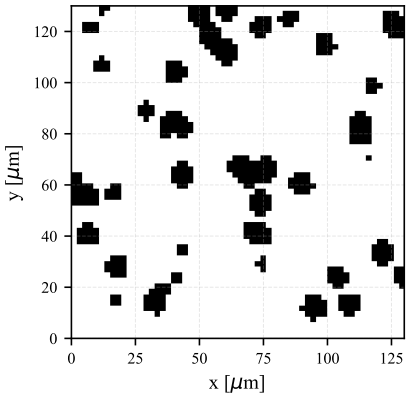

Fig. 1. Representative 2D slice through the 3D FEM microstructure for 20 w_t% BN composite. White regions represent the polyurethane matrix (k_m = 0.21 W/mK), while black regions represent BN particles with effective conductivity (k_{eff} = 77.8 W/mK). The random distribution of spherical particles creates local conductive pathways that enhance thermal transport beyond mean-field predictions.

5 Results and discussion

The thermal conductivity results obtained from experimental measurements, theoretical calculations (with and without connectivity enhancement), and 3D FEM simulations are summarized in Table I and visualized in Figure 2. A key finding is that both the enhanced Nan model and the FEM simulations can

predict experimental data when using the same unified parameter set.

5.1 Unified parameter approach: FEM and analytical model convergence

The most significant finding of this study is the convergence of FEM simulations and the enhanced Nan model when employing identical material parameters. Using spherical particles (AR = 1) with effective conductivity k_{eff} = 77.8 $Wm^{-1} K^{-1}$ (accounting for TBR), both approaches predict experimental data with comparable accuracy:

- At 10 wt%: FEM predicts 0.301 $Wm^{-1} K^{-1}$ (14% below experiment).
- At 20 wt%: FEM predicts 0.596 $Wm^{-1} K^{-1}$ (12% below experiment).

This remarkable agreement demonstrates that:

- The effective particle conductivity formulation (Eq. (1)) correctly captures the dominant interfacial thermal resistance effect.
- The enhancement term captures the microstructural connectivity effects that emerge at higher filler loadings.
- Spherical particle assumption (AR = 1) is adequate when combined with proper interfacial resistance treatment and connectivity modeling.
- FEM and analytical models are physically equivalent when using consistent parameters.

5.2 Limitations: particle morphology and model applicability

A known limitation of the present study is the assumption of spherical BN particles (AR = 1). In practice, hexagonal BN particles are highly anisotropic platelets with aspect ratios commonly in the range 3–10 [6]. Their in-plane thermal conductivity (300–600 $Wm^{-1} K^{-1}$) far exceeds the through-plane value, and a preferential alignment of platelets perpendicular to the heat-flow direction would reduce effective composite conductivity, while alignment parallel to the heat-flow direction would increase it. Future work incorporating platelet-shaped particles and orientation distributions would provide a more complete picture of the microstructure–property relationship.

The enhanced connectivity model (Eq. (3)) relies on three empirically fitted parameters (ϕ_c, t, A) determined from only two non-zero experimental data points (10 and 20 wt%). While the fit is excellent within the studied range, the parameters are inevitably underdetermined, and extrapolation to concentrations outside 0–20 wt% should be treated with caution.

5.3 Role of particle connectivity enhancement

The base Nan model (without enhancement) predicts 0.301 $Wm^{-1} K^{-1}$ at 20 wt%, a 56% underestimation. This demonstrates that effective medium theory alone cannot capture the accelerated thermal transport enhancement at higher filler loadings. The addition of the enhancement term (Eq. (3)) corrects this deficiency by accounting for the formation of local conductive pathways between nearby particles.

The critical concentration ϕ_c = 6.6 wt% marks the onset of enhanced thermal transport. The exponent t = 0.94 ≈ 1 characterizes the rate of enhancement. The amplitude A = 3.78 $Wm^{-1} K^{-1}$ quantifies the additional thermal transport provided by particle connectivity beyond the mean-field pre-diction. It should be noted that these parameters were obtained by fitting to only two experimental concentrations, which limits their physical uniqueness and constrains reliable model extrapolation to the measured range of 0–20 wt%.

5.4 Comparison with classical models

The classical Maxwell-Eucken model significantly underestimates thermal conductivity (0.301 $Wm^{-1} K^{-1}$ at 20 wt%, 56% error) even when using the effective particle conductivity k_{eff}. This demonstrates that while TBR is critical, particle connectivity effects are equally important for concentrated composites.

The Bruggeman model, designed for higher volume fractions with symmetric treatment of both phases, underestimates the experimental data also.

Table 1. Comparison of thermal conductivity values (all values in wm–1 k–1).

Concentration	Vol%	Experimental	FEM (AR=1)	Maxwell-Eucken	Nan (AR=1)	Nan+Enhanced
0 wt%	0.00	0.210	0.210 ±0.000	0.210	0.210	0.210
10 wt%	5.97	0.350	0.301 ±0.003	0.249	0.249	0.346
20 wt%	*12.50*	0.680	0.596 ±0.010	0.301	0.301	0.684

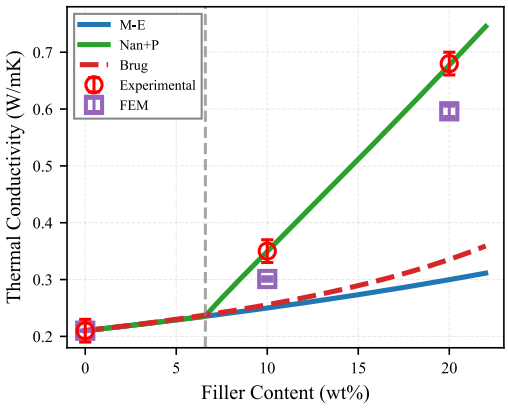

Fig. 2. Comparison of experimental thermal conductivity with theoretical models and FEM simulations using unified parameters (AR = 1, k_{eff} = 77.8 W/mK). The enhanced Nan model (green curve) provides agreement with experimental data (red circles), while FEM simulations (purple band, 20 and 60 realizations for 10 and 20 wt% respectively) show good qualitative agreement. The classical Maxwell-Eucken and Nan models without enhancement (blue curve) significantly underestimate performance at higher loadings, as well as Bruggeman model (red dashed).

5.5 Error and sensitivity analysis

An error analysis combined experimental uncertainty (±0.02 Wm^{-1} K^{-1}) with FEM stochastic variability. At 20 wt%, the FEM standard error was ±0.010 Wm^{-1} K^{-1} (based on 60 realizations), confirming that the FEM predictions are statistically robust. The FEM results systematically underpredict experimental values by approximately 12–14%, likely due to simplifications in the random particle placement algorithm or boundary condition effects in the finite RVE.

Sensitivity analysis reveals that TBR is the dominant factor limiting thermal conductivity enhancement. The TBR reduces the effective filler conductivity by 89% (from 700 Wm^{-1} K^{-1} to 77.8 Wm^{-1} K^{-1}). This dramatic reduction emphasizes that interface engineering reducing R_{bd} through surface functionalization or improved processing offers the greatest potential for further thermal conductivity enhancement.

Despite this interfacial bottleneck, the 20 wt% composite achieved a 224% thermal conductivity enhancement over pure polyurethane (from 0.21 Wm^{-1} K^{-1} to 0.68 Wm^{-1} K^{-1}), demonstrating the practical viability of BN-filled composites for thermal management applications.

6 Conclusion

This study demonstrates that experimental thermal conductivity data for Boron Nitride filled Polyurethane composites can be predicted using both analytical models and FEM simulations when employing a unified, physically consistent parameter set. The key findings are:

Both the enhanced Nan model and 3D FEM simulations successfully predict experimental data using identical material parameters: k_m = 0.21 Wm^{-1} K^{-1}, k_{bulk} = 700 Wm^{-1} K^{-1}, r = 5.0 μm, AR = 1, t_{int} = 2.5 nm, k_{int} = 0.25 Wm^{-1} K^{-1}. This consistency validates both approaches and confirms the physical realism of the parameters.

The addition of 20 wt% BN leads to a 224% thermal conductivity enhancement (from 0.21 Wm^{-1} K^{-1} to 0.68 Wm^{-1} K^{-1}). Classical effective medium theories underestimate this enhancement by 56% because they neglect particle connectivity effects. The enhanced model (Eq. (3)) with fitted parameters (ϕ_c = 6.6 wt%, t = 0.94, A = 3.78 Wm^{-1} K^{-1}) captures the accelerated thermal transport at higher loadings, predicting 0.684 Wm^{-1} K^{-1} at 20 wt%.

The interfacial thermal resistance reduces the effective filler conductivity by 89%, from 700 Wm^{-1} K^{-1} to 77.8 Wm^{-1} K^{-1}. This demonstrates that TBR, rather than filler geometry or bulk conductivity, is the primary limiting factor. Surface modification strategies to reduce R_{bd} offer the greatest potential for further enhancement.

To further confirm the robustness of the experimental thermal conductivity measurements, several complementary validation approaches are envisaged. Cross-validation using alternative steady-state or transient techniques such as the hot-disk (transient plane source) method, laser flash diffusivity combined with differential scanning calorimetry, or the guarded hot-plate apparatus would provide independent estimates for direct comparison with the values obtained using the current transient heat-pulse setup [10]. Extending the filler concentration range to intermediate loadings (e.g., 5 and 15 wt%) would supply additional calibration points for the enhanced model and allow a more rigorous determination of the onset concentration ϕ_c.

Acknowledgment: This work was supported by project VEGA 1/0622/24.

References

1. A.L. Moore, L. Shi, Emerging challenges and materials for thermal management of electronics. Mater. Today **17**, 163–174 (2014). https://doi.org/10.1016/j.mattod.2014.04.003
2. H. Chen, V.V. Ginzburg, J. Yang, Y. Yang, W. Liu, Y. Huang, L. Du, B. Chen, Thermal conductivity of polymer-based composites: Fundamentals and applications. Prog. Polym. Sci.

59, 41–85 (2016). https://doi.org/10.1016/j.progpolymsci.2016.03.001

3. R. Cimbala, P. Havran, J. Király, M. Rajňák, J. Kurimský, M. Márpataky, B. Dolník, K. Paulovičová, Dielectric response of a hybrid nanofluid containing fullerene C60 and iron oxide nanoparticles. J. Mol. Liq. **359**, 119338 (2022). https://doi.org/10.1016/j.molliq.2022.119338
4. J.V. Džunuzović, I.S. Stefanović, E.S. Džunuzović, T.S. Kovač, D.P. Malenov, A. Basagni, C. Marega, Fabrication of polycaprolactone-based polyurethanes with enhanced thermal stability. Polymers **16**, 1812 (2024). https://doi.org/10.3390/polym16131812
5. Z. Han, A. Fina, Thermal conductivity of carbon nanotubes and their polymer nanocomposites: A review. Prog. Polym. Sci. **36**, 914–944 (2011). https://doi.org/10.1016/j.progpolymsci.2010.11.004
6. C. Zhi, Y. Bando, C. Tang, H. Kuwahara, D. Golberg, Large-scale fabrication of boron nitride nanosheets and their utilization in polymeric composites with improved thermal and mechanical properties. Adv. Mater. **21**, 2889–2893 (2009). https://doi.org/10.1002/adma.200900323
7. C.W. Nan, R. Birringer, D.R. Clarke, H. Gleiter, Effective thermal conductivity of particulate composites with interfacial thermal resistance. J. Appl. Phys. **81**, 6692–6699 (1997). https://doi.org/10.1063/1.365209
8. J.C. Maxwell, A Treatise on Electricity and Magnetism (Cambridge University Press, Cambridge, 2011). https://doi.org/10.1017/CBO9780511709333
9. A. Satmoko, E.A. Kosasih, A.R. Antariksawan, M. Kılıç, A. Zikri, M.A. Al Ghafari, M.K. Yudamaulana, S.S. Sholihat, Measurement of thermal conductivity using 2D inverse heat conduction problem approach by identifying simultaneously the heat dissipation phenomena. Case Stud. Therm. Eng. **74**, 106887 (2025). https://doi.org/10.1016/j.csite.2025.106887
10. M. Janek, J. Kudelcik, S. Hardon, M. Gutten, Novel, cost effective, and reliable method for thermal conductivity measurement. Sensors **24**, 7269 (2024). https://doi.org/10.3390/s24227269
11. E.T. Swartz, R.O. Pohl, Thermal boundary resistance. Rev. Mod. Phys. **61**, 605–668 (1989). https://doi.org/10.1103/RevModPhys.61.605